High-order harmonic generation with a two-color laser pulse*

Luo Lao-Yong(罗老永), Du Hong-Chuan(杜洪川), and Hu Bi-Tao(胡碧涛)†

School of Nuclear Science and Technology, Lanzhou University, Lanzhou 730000, China

(Received 17 May 2011; revised manuscript received 23 July 2011)

We theoretically investigate the electron dynamics of the high-order harmonics generation process by combining a near-infrared 800 nm driving pulse with a mid-infrared 2000 nm control field. We also investigate the emission time of harmonics using time-frequency analysis to illustrate the physical mechanisms of high-order harmonic generation. We calculate the ionization rate using the Ammosov–Delone–Krainov model and interpret the variations in harmonic intensity for different control field strengths and delays. We find that the width of the harmonic plateau can be extended when the control electric field is added, and a supercontinuum from 198 to 435 eV is generated, from which an isolated 61-as pulse can be directly obtained.

Keywords: high-order harmonic generation, attosecond pulse

PACS: 32.80.Rm, 42.65.Ky, 42.65.Re **DOI:** 10.1088/1674-1056/21/3/033202

1. Introduction

The interactions of an intense laser pulse with atoms, molecule clusters and solids can lead to high-order harmonic generation (HHG). This forms two new physics research fields, strong field physics and nonlinear physics. HHG opens the possibility for a new source of coherent radiation in the extreme region,[1] and the recent applications of such coherent sources are now in progress.[2] HHG may be used as a table-top source of coherent ultrafast extreme-ultraviolet (XUV) radiation up to the water window spectral range.[3] The high-order harmonic spectrum generated by an intense laser field interacting with an atom or a molecule can be used to synthesize a single attosecond pulse or a train of attosecond pulses. Recent advances[4,5] have demonstrated that an isolated attosecond pulse can be generated by few-cycle driving pulses, polarization gating (PG) with a stabilized carrier phase,[6−8] and a two-color laser with an extreme ultraviolet attosecond pulse.[9] The tunable high-order harmonic is generated by controlling the quantum path.[10] The process of HHG can be well understood in terms of the semiclassical three-steps model:[11] first the electron tunnels through the barrier formed by the Coulomb potential and the laser field, then it oscillates quasi freely driven by the laser field and acquires the oscillation energy, and finally it recombines with the parent ion. During the recombination, a photon with energy equal to the ionization potential plus the kinetic energy of the recombining electron is emitted. The maximum photon energy is given by $E = I_{\rm p}+3.17U_{\rm p}$,[12] where $I_{\rm p}$ is the ionization potential of the atom, and $U_{\rm p}$ is the ponderomotive energy of the electron in the laser field. This equation implies that the harmonic cutoff can be extended through enhancing the intensity of the driving field. Thus it is interesting to expand the limiting cutoff law to the higher order.[13]

However, an extremely high driving field will lead to the ionization saturation of the target atom and limit the harmonic yields. On the other hand, the high ionization rate also leads to defocusing of the driving pulse and diphasing of the atomic dipole oscillators by the plasma, which then decreases the conversion efficiency.[14] In order to avoid the ionization-induced mismatching of the harmonics in the ionized medium, quasi-phase matching (QPM)[15,16] and nonadiabatic self-phase matching (NSPM)[17] are proposed. However, the unsatisfactory control abilities of both QPM and NSPM may limit their applications. Recently, it has been theoretically[18−21] and experimentally[22,23]

*Project supported by the National Natural Science Foundation of China (Grant Nos. 11075069, 91026021, and 11075068), the Fundamental Research Funds for the Central Universities, China (Grant No. lzujbky-2010-k08), and the Scholarship Award for Excellent Doctoral Student granted by the Ministry of Education, China.

†Corresponding author. E-mail: hubt@lzu.edu.cn

© 2012 Chinese Physical Society and IOP Publishing Ltd

shown that a mid-infrared driving pulse not only improves the harmonic conversion efficiency but also reduces the harmonic chirps, which is beneficial for attosecond pulse generation.[24] In our previous work, we proposed a method to generate a broadband supercontinuum by using a few-cycle two-color laser pulse and a high-order pulse, from which an isolated 24-as pulse could be directly obtained.[25]

In this work, we propose a method to generate a broadband supercontinuum, from which an isolated 61-as pulse can be obtained directly. The combination of a near-infrared driving field and a mid-infrared control field is adopted. The harmonic spectrum is obviously extended. By accurately adjusting the carrier-envelop phase (CEP), the delay between the driving and the control fields, and the intensity of the control field, the modulations become much more indiscernible, which is conducive to the generation of an attosecond pulse. The ionization probability of an He is also estimated, by using the Ammosov–Delone–Krainov (ADK) model, to be below 0.8%, which allows us not only to apply the most appropriate phase-matching technique, but also to employ an energy scaling scheme.

2. Theoretical model

In our calculation, the Lewenstein model[26] is used to qualitatively give the harmonic spectrum in the two-color field. In this model, the instantaneous dipole moment of an atom is described as (in atomic units)

$$\begin{aligned} d_{nl} = {} & \mathrm{i}\int_{-\infty}^{t}\mathrm{d}t'\left[\frac{\pi}{\varepsilon+\mathrm{i}(t-t')/2}\right]^{3/2} \\ & \times d^{*}\left[p_{\mathrm{st}}(t',t)-A(t)\right]d\left[p_{\mathrm{st}}(t',t)-A(t')\right] \\ & \times \exp[-\mathrm{i}\,S_{\mathrm{st}}(t',t)]E_{\mathrm{f}}(t')g(t')+\mathrm{c.c.}, \end{aligned} \tag{1}$$

where $E_{\mathrm{f}}(t)$ is the electric field of the laser pulse, $A(t)$ is its associated vector potential, and ε is a positive regularization constant. p_{st} and S_{st} are the stationary momentum and the quasiclassical action, respectively, which are given by

$$p_{\mathrm{st}}(t',t) = \frac{1}{t-t'}\int_{t'}^{t}A(t'')\mathrm{d}t'', \tag{2}$$

$$\begin{aligned} S_{\mathrm{st}}(t',t) = {} & (t-t')\,I_{\mathrm{p}}-\frac{1}{2}p_{\mathrm{st}}(t',t)(t-t') \\ & +\frac{1}{2}\int_{t'}^{t}A^{2}(t'')\mathrm{d}t'', \end{aligned} \tag{3}$$

where I_{p} is the ionization energy of the atom, and $d(p)$ is the dipole matrix element for the transition from the ground state to the continuum state. For hydrogen-like atoms, $d(p)$ can be approximated by

$$d(p) = \mathrm{i}\,\frac{2^{7/2}}{\pi}(2I_{\mathrm{p}})^{5/4}\frac{p}{(p^{2}+2I_{\mathrm{p}})^{3}}. \tag{4}$$

The $g(t)$ in Eq. (1) represents the ground-state amplitude and is given by

$$g(t') = \exp\left[-\int_{-\infty}^{t}\omega(t')\mathrm{d}t'\right], \tag{5}$$

where $\omega(t)$ is the ionization rate and is calculated by the ADK tunneling model as[27]

$$w(t) = \omega_{\mathrm{p}}\left|C_{n^{*}}\right|^{2}\left(\frac{4\omega_{\mathrm{p}}}{\omega_{t}}\right)^{2n^{*}-1}\exp\left(-\frac{4\omega_{\mathrm{p}}}{3\omega_{t}}\right), \tag{6}$$

with

$$\begin{aligned} & \omega_{\mathrm{p}} = \frac{I_{\mathrm{p}}}{\hbar}, \quad \omega_{t} = \frac{e\left|E_{\mathrm{f}}(t)\right|}{\sqrt{2m_{\mathrm{e}}I_{\mathrm{p}}}}, \quad n^{*} = Z\left(\frac{I_{\mathrm{ph}}}{I_{\mathrm{p}}}\right)^{1/2}, \\ & \left|C_{n^{*}}\right|^{2} = \frac{2^{2n^{*}}}{n^{*}\Gamma(n^{*}+1)\Gamma(n^{*})}, \end{aligned} \tag{7}$$

Z being the net resulting charge of the atom, I_{ph} the ionization potential of the hydrogen atom, and e and m_{e} the electron charge and the electron mass, respectively.

The harmonic spectrum can then be obtained, which is proportional to the squared modulus of the Fourier transform of $a(t)$

$$P_{A}(\omega) = \left|\frac{1}{\sqrt{2\pi}}\int_{0}^{T_{\mathrm{l}_0}}a(t)\,\mathrm{e}^{-\mathrm{i}\,\omega t}\mathrm{d}t\right|^{2}, \tag{8}$$

where $a(t)$ is the dipole acceleration $a(t) = \ddot{d}_{nl}(t)$, and T_{l_0} is the duration of the laser pulse.

3. Results and discussion

In our simulation, the electrical field can be expressed as

$$\begin{aligned} E(t) = {} & E_{0}f_{0}(t)\cos(\omega_{0}t+\phi_{\mathrm{CEP}}) \\ & +E_{1}f_{1}(t-\tau)\cos(\omega_{1}(t-\tau)), \end{aligned} \tag{9}$$

with

$$f_{0} = \sin^{2}\left(\frac{\pi t}{5T_{0}}\right), \quad f_{1} = \sin^{2}\left(\frac{\pi t}{2T_{1}}\right), \tag{10}$$

where E_i, f_i, ω_i and T_i $(i = 0, 1)$ are the peak amplitudes, envelopes, frequencies and optical cycles of the driving pulse and the control field, respectively, τ is the time delay between the driving pulse and the

control field and is set to be $0.05T_0$, and $\Phi_{\rm CEP}$ is the carrier-envelope phase of the driving pulse and is set to be π throughout this paper.

In order to demonstrate our scheme, we first investigate the HHG process in terms of the semiclassical three-step model,[11] which gives a clear physical picture. In our calculation, we choose $\omega_0 = 0.057$ a.u. (a.u. stands for arb. units) and $\omega_1 = 0.4\omega_0$ corresponding to $\lambda_0 = 800$ nm and $\lambda_1 = 2000$ nm, respectively, which can be produced from a Ti:saphire laser system via an optical parametric amplifier (OPA), $T_{1_0} = 551$ a.u. corresponds to a duration (full width at half maximum (FWHM)) of 5 fs, and the intensities of the driving and control fields are set to be 0.18 and 0.04 a.u., respectively.

The electron dynamics of the HHG process and the ionization rate calculated by the ADK model[27] in the driving pulse and in the composed field are shown in Figs. 1 and 2, respectively. Because the harmonic efficiency is determined mainly by the ionization rate (the ground state population is not fully depleted), the HHG process can be well depicted in terms of classical electron trajectories. Here we present the electron trajectory as a function of ionization time and recombination time. In Fig. 1(a), we present the electric field of the driving pulse, and, as shown in Fig. 1(b), there are many peaks (marked as P_1, P_2 and P_3) of trajectories in the laser field. The difference between the highest (P_2) and the second highest (P_3) half-cycle photon energies is so small that the bandwidth of the supercontinuum[28] is only 27 eV. In Fig. 2(a), the driving, the control and the synthesized electric fields are each shown as a function of time. By adding the control field to the fundamental driving field, the shape of the electric field is changed, leading to the expansion of the absolute value of the peak. Figure 2(b) shows the electron kinetic energy as a function of ionization and recombination time, and the ionization probability calculated by the atomic ADK model, with the two-color field shown in Fig. 2(a). Obviously, in this case, the ionization probability shown in Fig. 2(b) is much higher than that in Fig. 1(b). This result indicates that the two-color excitation scheme increases the ionization rate. Moreover, in Fig. 2(b) we can clearly see that the second and third ionization peaks are successfully suppressed. The contribution of quantum path P_1' to the HHG can be ignored due to its extremely low ionization rate. Then the bandwidth of the supercontinuum is directly determined by the energy difference between P_2' and P_3', which contributes to the supercontinuum generation. Thus, a supercontinuum with a bandwidth of 237 eV can be obtained.

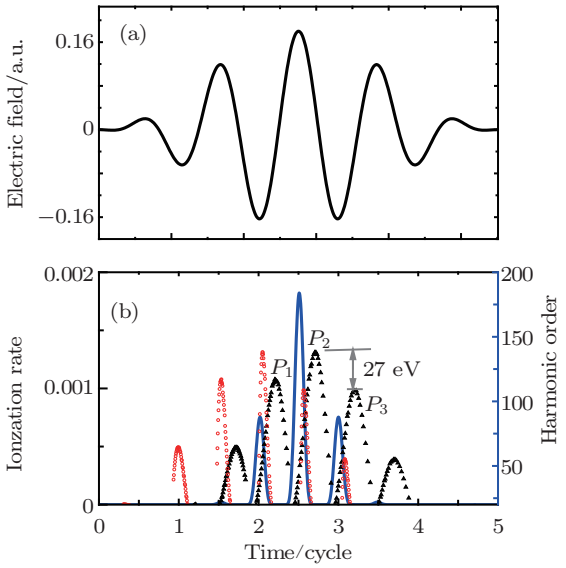


Fig. 1. (colour online) (a) The electric field of the fundamental driving pulse, and (b) the dependence of the electron kinetic energy on ionization time (○) and recombination time (▲), and the dependence of the ionization probability on time (black line).

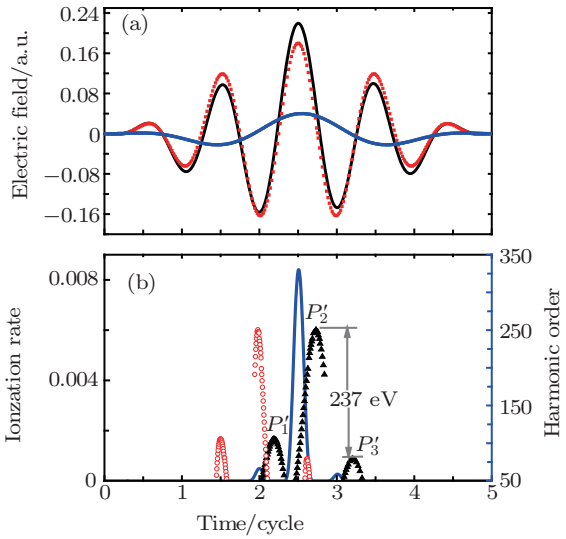


Fig. 2. (colour online) (a) The synthesized laser field (black solid line) of the fundamental driving laser pulse (short dotted line) in combination with a low-frequency laser pulse (short dashed line), and (b) the dependence of the electron kinetic energy on ionization time (○) and recombination time (▲) with the driving field, and the dependence of the ionization probability (solid line) on time.

We investigate the harmonic spectrum using the Lewenstein model[13] to confirm our prediction. The parameters are the same as those in Fig. 2(b), and the harmonic spectrum in the two-color field is shown in Fig. 3(a) (black solid line). For comparison, the harmonic spectrum in the 800 nm laser field is also given

(dotted black line). As shown in the figure, the harmonics from 198 eV to the cut off (435 eV) become continuous. But the harmonic yield of the generated supercontinuum is about one-order lower than that of the same order harmonics in the 800 nm driving pulse. The bandwidth of the supercontinuum is determined directly by the energy difference between P_2' and P_3'. The time-frequency distribution[29] of the HHG shown by the solid curve in Fig. 3(a) is also presented in Fig. 3(b) to further understand the harmonic spectrum. It is clear that three peaks contribute to the harmonics, and the branch (short quantum path) under the highest peak is much more dominant than the upper one, resulting in the broadband supercontinuum of the plateau in Fig. 3(a). These results accord well with those obtain from the classical approaches shown in Fig. 2(b).

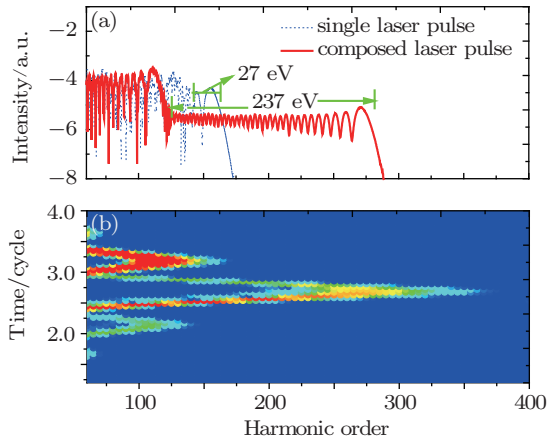


Fig. 3. (colour online) (a) Harmonic spectra in the few-cycle fundamental driving pulse (short dashed line) and in the synthesized laser pulse (solid line), and (b) their time-frequency distribution in the two-color laser field.

The sensitivity of the harmonic spectrum to the variation of electric field E_1 of the control pulse is investigated. The result is shown in Fig. 4(a). The harmonic spectra with $E_1 = 0.02$ a.u. (short dotted line), 0.04 a.u. (short dashed line) and 0.06 a.u. (blue solid line) are shown. They reveal that the bandwidth of the supercontinuum increases with the increase in the electric field E_1 of the control pulse, because the recombination kinetic energy increases with the increase in E_1. On the other hand, the ionization rate in peak P_2' is successfully suppressed by the increasing pulse. Thus, the harmonic yield of the generated supercontinuum decreases with the increase in electric field E_1 of the control pulse. We can modulate not only the duration but also the intensity of the harmonic generation. This implies that we can obtain the most appropriate harmonic spectrum in a reasonable laser field. Moreover, the modulation of the supercontinuum is due to the interference of the short and long quantum paths. For the two-color field, the short quantum path becomes more and more dominant with the increase in the control field. So the modulations become much more indiscernible, as shown in the inset of Fig. 4(a), which is more conducive to producing the attosecond pulse. We also investigate the harmonic spectra with different values of τ; the harmonic spectra with $\tau = 0.0T_0$, $0.05T_0$ and $0.25T_0$ are given for comparison. Figure 4(b) reveals that the bandwidth of the supercontinuum decreases with the increase in time delay. Thus, it is important to accurately control the delay of the two-color field to obtain the broad supercontinuum.

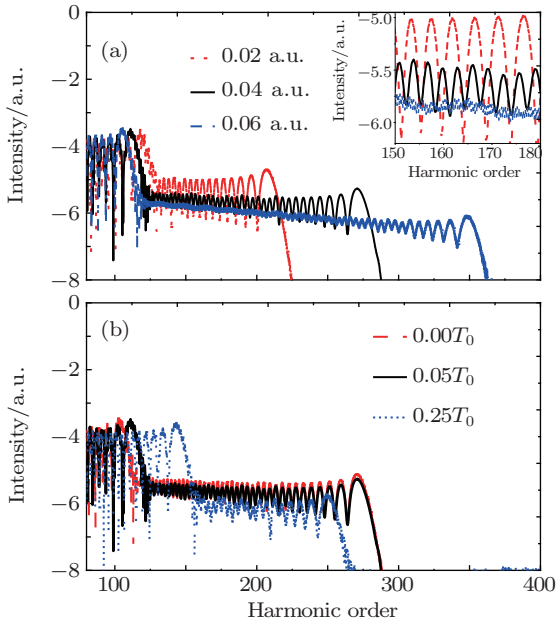


Fig. 4. (colour online) HHG spectra with (a) different laser pulse intensities and (b) different pulse delays. The insert shows the enlarged spectra of the middle harmonic order.

Now we further calculate the attosecond pulse generation in the two-color field. Figure 5 shows the temporal profiles of the isolated attosecond pulses generated by the harmonics with different central frequencies. The parameters are the same as those in Fig. 2(a). As shown in Fig. 5, by adding a frequency window with a bandwidth (61 eV) of 40-order harmonics to the supercontinuum, isolated attosecond pulses with tunable wavelengths can be obtained directly without any chirp compensation. And we can see in Fig. 3(a) that during the supercontinuum generation time, the intensity of the harmonic order decreases with the increase in harmonic order time. So the intensity of the attosecond pulse gradually reduces

as the central wavelength decreases. The duration of the attosecond pulse hardly changes with the increase in central frequency, though the intensity decreases. This reveals that the pulse duration is not sensitive to the position of the frequency window. The isolated attosecond pulse with tunable wavelength can be used in many fields, such as nanolithography, high-resolution tomography and XUV interferometry.

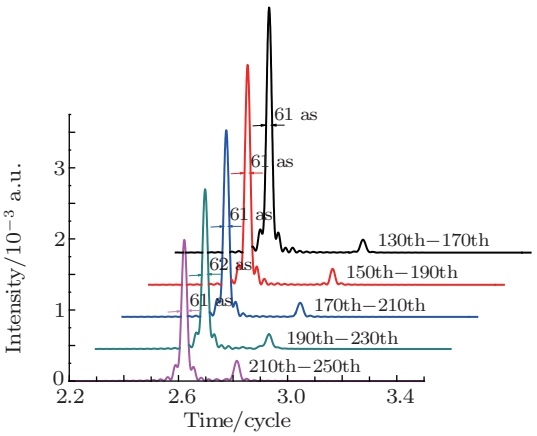


Fig. 5. (colour online) Temporal profiles of the isolated attosecond pulses by synthesizing the harmonics of 130th–170th, 150th–190th, 170th–210th, 190th–230th and 210th–250th.

4. Conclusion

We studied the generation of high harmonics and isolated attosecond pulses by combining a near-infrared 800 nm driving pulse with a mid-infrared 2000 nm control pulse. The result reveals that the control laser pulse can simultaneously modulate the acceleration and the ionization steps of the HHG. We clearly demonstrate the electronic dynamic mechanism of the harmonic generation, and by adjusting the intensity and the time delay of the control field to enhance one quantum path and suppress the other, we control high-order harmonic generation. So we can control not only the bandwidth, but also the yield of the supercontinuum, from which an isolated 61-as pulse can be directly obtained. On the other hand, we can adjust the control field to make the modulation become much more indiscernible, which is more beneficial to the generation of the attosecond pulse. The ionization probability of He is also estimated by the ADK model to be below 0.8%, which allows us not only to apply the most appropriate phase-matching technique, but also to employ an energy scaling scheme.

References

[1] Spielmann C, Burnett N H, Sartania S, Koppitsch R, Schnerer M, Kan C, Lenzner M, Wobrauschek P and Krausz F 1997 *Science* **278** 661
[2] Chang Z, Rundquist A, Wang H, Murnane M M and Kapteyn H C 1997 *Phys. Rev. Lett.* **79** 2967
[3] Hentschel M, Kienberger R, Spielmann C, Reider G A, Milosevic N, Brabec T, Corkum P, Heinzmann U, Drescher M and Krausz F 2001 *Nature* **414** 509
[4] Yao J, Li Y, Zeng B, Xiong H, Xu H, Fu Y, Chu W, Ni J, Liu X, Chen J, Cheng Y and Xu Z 2010 *Phys. Rev.* A **82** 023826
[5] Christov I P, Murnane M M and Kapteyn H C 1997 *Phys. Rev. Lett.* **78** 1251
[6] Chang Z 2005 *Phys. Rev.* A **71** 023813
[7] Du H and Hu B 2010 *Opt. Express* **18** 25966
[8] Feng X, Gilbertson S, Mashiko H, Wang H, Khan S D, Chini M, Wu Y, Zhao K and Chang Z 2009 *Phys. Rev. Lett.* **103** 183901
[9] Zhang G, Wu J, Xia J and Liu X 2009 *Phys. Rev.* A **80** 055404
[10] Zeng Z, Cheng Y, Fu Y, Song X, Li R and Xu Z 2008 *Phys. Rev.* A **77** 023416
[11] Corkum P B 1993 *Phys. Rev. Lett.* **71** 1994
[12] McPherson A, Gibson G, Jara H, Johann U, Luk T S, McIntyre I A, Boyer K and Rhodes C K 1987 *J. Opt. Soc. Am.* B **4** 595
[13] Chang Z, Rundquist A, Wang H, Margaret M M and Henry C K 1997 *Phys. Rev. Lett.* **79** 2967
[14] Hong W, Zhang Q, Yang Z and Lu P 2009 *Phys. Rev.* A **80** 053407
[15] Paul A, Bartels R A, Tobey R, Green H, Welman S, Christov I P, Murnane M M, Kapteyn H C and Backus S 2003 *Nature* **421** 51
[16] Zheng L, Chen X, Tang S and Li R 2007 *Opt. Express* **15** 17985
[17] Seres E, Seres J, Krausz F and Spielmann C 2004 *Phys. Rev. Lett.* **92** 163002
[18] Tate J, Auguste T, Muller H, Salieres P, Agostini P and DiMauro L F 2007 *Phys. Rev. Lett.* **98** 013901
[19] Du H, Wang H and Hu B 2011 *Chin. Phys.* B **20** 044207
[20] Ye X, Zhou X, Zhao S and Li P 2009 *Acta Phys. Sin.* **58** 1579 (in Chinese)
[21] Guo Y, Lu R, Han K and He G 2009 *Int. J. Quant. Chem.* **109** 3410
[22] Takahashi E, Kanai T, Ishikawa K, Nabekawa Y and Midorikawa K 2008 *Phys. Rev. Lett.* **101** 253901
[23] Doumy G, Wheeler J, Roedig C, Chirla R, Agostini P and DiMauro L F 2009 *Phys. Rev. Lett.* **102** 093002
[24] Kienberger R, Goulielmakis E, Uiberacker M, Baltuska A, Yakovlev V, Bammer F, Scrinzi A, Westerwalbesloh T, Kleineberg U, Heinzmann U, Drescher M and Krausz F 2004 *Nature* **427** 817
[25] Du H, Wang H and Hu B 2010 *Phys. Rev.* A **81** 063813
[26] Lewenstein M, Balcou P, Yu M I, L'Huillier A and Corkum P B 1994 *Phys. Rev.* A **49** 2117
[27] Ammosov M V, Delone N B and Krainov V P 1986 *Sov. Phys. JETP* **64** 1191
[28] Zhang Q, Lu P, Lan P, Hong W and Yang Z 2008 *Opt. Express* **16** 9797
[29] Antoine P, Piraux B and Maquet A 1995 *Phys. Rev.* A **51** R1750